International Journal of Thermophysics (2023) 44:34
https://doi.org/10.1007/s10765-022-03144-4

Surface Tension of Ethylene Glycol-Based Nanofluids Containing Three Types of Oxides: Zinc Oxide (ZnO), Magnesium Oxide (MgO) and Indium Oxide (In_2O_3)

Julian Traciak[1] · **Gaweł Żyła**[1]

Received: 14 November 2022 / Accepted: 12 December 2022 / Published online: 2 January 2023

Abstract

The paper presents the results of an experimental study of the density and surface tension of ethylene glycol-based nanofluids containing zinc oxide, magnesium oxide and indium oxide. Du Noüy ring method was employed to determine the values of the surface tension of these nanofluids. Samples were prepared in various mass fractions from 0.01 to 0.05 with 0.01 step. Examination was performed in the temperature range from 283.15 K up to 318.15 K. The averaged surface tension values for the studied ZnO14-EG, ZnO25-EG, MgO-EG, In_2O_3-EG nanofluids at 298.15 K are 48.685, 48.471, 48.335, and 48.462 $mN{\cdot}m^{-1}$, respectively. It was presented that surface tension value could be consider as constant within the examined mass fraction of the particles, and the explanation of such behaviour was provided.

Keywords Density · Ethylene glycol · Indium oxide · Magnesium oxide · Nanofluid · Surface tension · Zinc oxide

Nomenclature

A, B, C	Eq. 1 coefficients
e	Euler's number [–]
p	Pressure [Pa]
T	Temperature [K]
u_r	Relative uncertainty [–]
γ	Surface tension [$mN{\cdot}m^{-1}$]
ρ	Density [$kg{\cdot}m^{-3}$]
φ	Fraction [–]

✉ Gaweł Żyła
gzyla@prz.edu.pl

Julian Traciak
jtraciak@prz.edu.pl

[1] Department of Physics and Medical Engineering, Rzeszow University of Technology, al. Powstańców Warszawy 6, Rzeszow 35-959, Poland

subscripts

bf	Base fluid
m	Mass
nf	Nanofluid
v	Volume

Abbreviations

EG	Ethylene glycol
LSTM	Long-short term memory
CNN-LSTM	Convolutional neural network with long-short term memory
SEM	Scanning electron microscope
TPCT	Two-phase closed-loop thermosyphon

1 Introduction

Since the early 1990s, scientists have begun to explore nanomaterial technology for heat transfer applications. Nanofluids are suspensions of nanoparticles in base fluids, such as water, oil or alcohol, designed to improve thermophysical properties over the base fluids themselves [1]. Among other applications, they can be used in heat transfer systems by reducing their size and increasing the performance of these systems. Applications of nanofluids are promising in automotive, construction, microelectronics, energy and other fields, and are becoming a hot spot for research in materials, physics and chemistry as it was presented in recent review papers focused on this issue [2–10].

Zinc oxide in ethylene glycol (ZnO-EG) nanofluids were studied for rheological and thermal properties. Yu et al. [11] showed that the thermal conductivity of nanofluids strongly depends on the size of the suspended nanoparticles. In their work, they presented a non-linear increase in thermal conductivity with increasing volume fraction of nanoparticles. The maximum increase was 45%, and it was recorded for a concentration of 6.9 vol%. They also investigated the rheological properties of ZnO-EG nanofluids. The results showed that these materials with low volume concentrations ($\varphi_v \leq 2$ vol%) exhibit Newtonian behaviour, with viscosity decreasing significantly with increasing temperature. In contrast, at higher volume concentrations ($\varphi_v \geq 3$ vol%), shear-shear behaviour is observed, exhibiting non-Newtonian behaviour. The same conclusions were reached by Pastoriza et al. [12], studying the same nanofluids. However, in their results, they presented a 26.5% increase in thermal conductivity for a concentration of 5 vol% Suganthi et al. [13], presented the effect of nanoparticle concentration and temperature on the thermal conductivity and viscosity of ZnO-EG and ZnO-EG-water nanofluids. Their study showed an increase in thermal conductivity and a decrease in viscosity. It was presented that ZnO-EG and ZnO-EG-water nanofluids showed an increase in thermal conductivity of 33.4% and 17.26% and a decrease in viscosity of 39.2% and 17.34% at particle volume concentrations of 4 and 2 vol%, respectively. In the work of Li et al. [14], ZnO-EG nanofluids with a mass concentration of 10.5 wt% exhibit Newtonian behaviour, while the viscosity decreases with increasing temperature and increases with increasing mass concentration. Demirpolat et al. [15] in their work

showed that heat flow coefficients can be estimated using the LSTM and CNN-LSTM deep learning model for ZnO-EG nanofluids.

In the literature, publications on magnesium oxide nanofluids in ethylene glycol (MgO-EG) also can be found. Xie et al. [16] prepared MgO-EG nanofluids and investigated their properties, including thermal conductivity and viscosity. They showed that the increase in thermal conductivity increases non-linearly with the addition of nanoparticles. The value of the increase compared to the base fluid was 40.6% for a volume fraction of 0.05. Hemmat et al. [17] conducted an experimental study to investigate the effect of particle size on the thermal conductivity of MgO-EG nanofluids in the temperature range from 298.15 K to 328.15 K and volume concentrations up to 5%. They found that the effect of temperature on increasing the thermal conductivity was less than that of particle size and concentration. It was revealed that for low concentrations the change in nanoparticle size was not significant, while at high volume concentrations, namely 5 %, with a change in particle size from 60 nm to 20 nm, the increase in thermal conductivity was approximately 8 to 10 %. The paper by Adioet al. [18] presents experimental measurements on the behaviour of the pH and electrical conductivity of MgO-EG nanofluid as a function of temperature variation, nanoparticle size, volume fraction and sonification time and energy. Both pH and electrical conductivity of the nanofluid increased with decreasing particle size. However, sonification time and energy showed no effect on the electrical conductivity and pH of the MgO-EG nanofluid samples. Only temperature, volume fraction and nanoparticle size showed an effect on the studied thermophysical properties of MgO-EG nanofluids. In a later paper, Adio et al. [19] investigated the viscosity of MgO-EG nanofluids and showed that it decreased exponentially with increasing temperature and increased linearly with increasing volume fraction. Żyła et al. [20] showed that the viscosity of the magnesium oxide-ethylene glycol nanofluid increased with increasing volume fraction of nanoparticles in suspension. At the same time, they confirmed that the material exhibits a Newtonian character. A comparison of MgO-EG nanofluids with pure ethylene glycol from the point of view of advantages for flow applications shows that a nanofluid with a particle volume fraction of 0.052 presents the best heat transfer properties.

In the literature, there are just a few papers on selected properties of indium oxide nanofluids in ethylene glycol (In_2O_3-EG). One of these is the work of Fal et al. [21] in which they found an increase in the electrical conductivity of these nanofluids with both concentration and temperature. The maximum increase in electrical conductivity of In_2O_3-EG nanofluids, 27 300% was detected for a volume fraction of 0.0081 at 333.15 K. Żyła et al. [22] presented the results of an experimental study of the dynamic viscosity of indium oxide nanofluids in ethylene glycol and found that these materials exhibit Newtonian character for each nanoparticle fraction tested. They presented in their results that viscosity increases with nanoparticle fraction, and showed that temperature has a strong influence on the viscosity of these materials.

In summary, it can be seen that such papers focused on thermophysical properties of ZnO-EG, MgO-EG and In_2O_3-EG nanofluids have been presented, but no one has yet investigated the surface tension according to the best authors knowledge.

Nanofluid properties, such as surface tension and wettability, have an important role in estimating heat transfer or thin film flows, as presented in details in Ref. [23]. Surface tension plays an important role in many heat transfer applications.

In heat transfer devices, such as heat pipes, correlations to predict heat flow require knowledge of surface tension [24]. To describe the operation of these devices, Weber's number is used, which is a convenient measure of the probability of liquid entrainment, whereas Weber's number increases as the surface tension decreases. In two-phase closed-loop thermosyphons (TPCTs), surface tension also affects their effective operation. In a thermosyphon evaporator, the peak heat flux can be determined by the dimensionless Kutateladze number [25], which is usually related to the Bond number function [26]. A decrease in surface tension causes an increase in capillary number, which is associated with boiling flow in microchannels [27]. The above and additional parameters that are also affected by surface tension are described in detail in Ref [23].

Despite this important role, the study of surface tension remains outside the mainstream study of nanofluid properties. Of the nanofluids based on ethylene glycol as a base fluid, surface tension values have so far been investigated for SiO_2-EG [28], TiO_2-EG [29], ZrO_2-EG [30], ZnO-EG [31], AlN-EG, Si_3N_4-EG, TiN-EG [32, 33], Cu-EG [34], Bi_2O_3-EG [34], MWCNT-EG [35]. Additionally in the Ref. [36] the surface tension of In_2O_3-EG, ZnO-EG at low mass concentrations (from 0 wt% to 1 wt%) at 298.15 K was presented. The present work is intended to be an extension of the experimental studies included in the previous works. Finally, the results presented here confirms a semi-empirical model of surface tension of nanofluids that has been presented elsewhere [36].

In this experimental work, the surface properties of In_2O_3-EG, MgO-EG and ZnO-EG nanofluids with mass concentration change from 1 wt% to 5 wt% at the temperature range of 283.15 K to 318.15 K were investigated to fill this gap in nanofluids research.

2 Materials and Methods

This section presents the materials used in this work as well as the entire process for the preparation of the tested nanofluid samples. In addition, the measurement methods and their relative uncertainties values are described here.

2.1 Nanoparticle Characterisation

All nanoparticles used in this study were manufactured by PlasmaChem GmbH (Berlin, Germany) and are commercially available.

The zinc oxide nanoparticles used in this work are in the form of a dry, white powder. Two sizes of nanoparticles 14 nm and 25 nm were used in this work, further labelled ZnO14 and ZnO25, respectively. ZnO14 are zinc oxide nanoparticles for which the manufacturer claims an average nanoparticle size of 14 nm, as well as a purity above 99%. For ZnO25, on the other hand, the average nanoparticle size declared by the manufacturer is 25 nm, also with a purity above 99%. The manufacturer declared specific surface area for ZnO14 is 30 ± 5 $m^2 \cdot g^{-1}$ and for ZnO25 is 19 ± 5 $m^2 \cdot g^{-1}$. Figure 1 shows SEM images of ZnO nanoparticles confirming the size declared by the manufacturer.

The magnesium oxide nanoparticles are in the form of a white powder with a purity of more than 99%. The manufacturer's declared average particle size is 20 nm

and the specific surface area is approximately 50 $m^2 \cdot g^{-1}$. A scanning electron microscope (SEM) image of the dry MgO nanoparticles was taken using a VEGA3 microscope (TESCAN Brno, s.r.o., Brno, Czech Republic). The SEM image confirms the claimed size of the nanoparticles and can be found elsewhere [20].

The In_2O_3 nanoparticles used are in the form of a dry, light yellow powder. The average size of the indium oxide nanoparticles as declared by the manufacturer is 4 nm and was confirmed using a JEOL JSM-6700F field emission scanning electron microscope (SEM) (JEOL, Tokyo, Japan), and the images taken on it can be found elsewhere [21].

2.2 Sample Preparation

In the experiments ethylene glycol (EG), with purity over 99% produced by Fisher Chemical (Loughborough, UK), was employed as a base fluid. All the nanofluids produced for this work were prepared in 50 ml vials using the two-step method. In this method, in the first step, the nanoparticles are mechanically mixed with the base fluid to obtain a heterogeneous suspension with a low degree of nanoparticle dispersion. In such a suspension, there are agglomerates of nanoparticles that quickly sediment. In order to counteract this phenomenon and to better disperse the nanoparticles and obtain a homogeneous mixture, a second stirring by means of ultrasound is introduced. For the purpose of this work, no surfactants were used during the preparation of the nanofluid samples. Nanofluids with mass concentrations in the range from 1 wt% to 5 wt% with 1 wt% step were produced.

The process of preparing the nanofluids started with weighing the appropriate amount of nanoparticles on an analytical balance (Pioneer Semi-Micro PX225DM, OHAUS Corporation, Parsippany, NJ, USA), followed by the addition of ethylene glycol to obtain the desired mass concentration. The prepared nanofluids were premixed mechanically on an IKA Vortex 3 shaker (IKA, Staufen, Germany) for 30 min. Then, in order to obtain a homogeneous mixture, the nanofluids were additionally mixed using ultrasound in an Emmi 60 HC ultrasonic cleaner (EMAG,

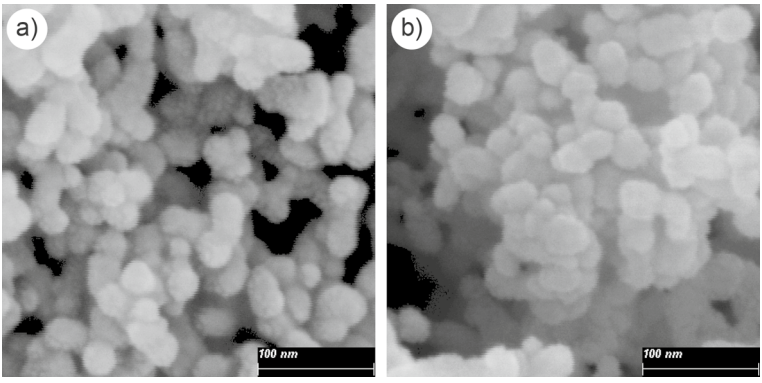

Fig. 1 Scanning electron microscope (SEM) pictures of dry zinc oxide (ZnO) nanopowders: (a) ZnO14, (b) ZnO25

Moerfelden-Walldorf, Germany) with a power of 450 W and a frequency of 45 kHz for 200 min while eliminating agglomerates and removing air bubbles. The sample preparation process was completed using a Sonics Vibracell VCX130 high-energy ultrasound generator (Sonics & Materials Inc, Newtown, USA) for 5 min.

Taking into account the accuracy of the analytical balance, the uncertainty of mass fraction was determined to be 2% of the presented value.

The stability of the nanofluids studied is determined not quantitatively but qualitatively. Based on the visual observation ZnO-EG, MgO-EG, and In_2O_3-EG nanofluids were stable for 6, 24, and 8 h, respectively. After this time sedimentation occurs.

The nanofluid samples prepared in this way were immediately tested for both density and surface tension values. All samples were stable during the measurements.

2.3 Mass Density Measurements

In order to correctly determine the surface tension of nanofluids, it is necessary to know their mass density. For the purpose of this work, nanofluid density values were measured for all nanofluids that were produced and used. The density values obtained are used to accurately determine the Zuidemia-Waters [37] correction factor, in order to best describe the surface tension.

Mass density measurements were carried out using an automatic oscillating U-tube densitometer DMA 4100 M (Anton Paar, Graz, Austria). The instrument was calibrated using deionised water at atmospheric pressure and a temperature of 293.15 K. All samples were measured over the temperature range from 283.15 K to 318.15 K. Mass density measurements comprised three measurement series, with ten measurements in each series, for all nanofluids tested. The uncertainty of the measurement values obtained with this device was determined by the deviation between the experimental data and the literature value and the standard deviation of one hundred measurements of the density of distilled water at 298.15 K. For one hundred measurements, the distilled water density obtained is 0.9969 g cm^{-3} with a standard deviation of 0.0002 g cm^{-3}. The literature value of [38] for the density of water at 298.15 K is 0.997066^{-3} with a standard deviation of 0.000001 g cm^{-3}. Referring to the literature values and the experimental results obtained, the relative uncertainty of the density measurements can be determined to be 0.1%.

2.4 Surface Tension Measurements

The PI-MT1A.KOM tensiometer (Polon-Izot, Warsaw, Poland) was used to determine the surface tension values of nanofluids for this work. This tensiometer uses the Du Noüy ring method. Measurement with this technique involves immersing a thin ring in the liquid and then pulling it out at a constant speed until it is detached from the sample. Figure 2 shows the measurement process using this method. The diagram shows the position of the ring in relation to the liquid under test and how this changes the measured value of the surface tension.

In order to determine the surface tension values of the test samples, three series of ten measurements were carried out for each nanofluid sample, and the values presented are the arithmetic averages of these series.

To determine the uncertainty of the surface tension measurements carried out with this device, ten measurements of pure ethylene glycol at 298.15 K were made. A result of 47.49 $mN{\cdot}m^{-1}$ with a standard deviation of 0.03 $mN{\cdot}m^{-1}$ was obtained, which is in agreement with the literature values of 48.02 $mN{\cdot}m^{-1}$ [38], 48.07 $mN{\cdot}m^{-1}$ [39], 47.89 $mN{\cdot}m^{-1}$ [40]. Taking all of these factors into account, the relative uncertainty of the surface tension measurements was determined to be 1%.

3 Results

In this section, the results of measurements of fundamental physical properties of ZnO-EG, MgO-EG and In_2O_3-EG nanofluids at the temperature range of 283.15 K to 318.15 K were presented and discussed.

3.1 Mass Density

The results of density measurements of all mass concentrations of the ZnO14-EG, ZnO25-EG, MgO-EG and In_2O_3-EG nanofluids are shown in Fig. 3. All the density values obtained for the nanofluids tested are also presented in the tables in Appendix 1.

The mass density increases linearly with increasing nanoparticle mass fraction for all tested nanofluids, which may confirm their uniform dispersion. At the same time, a linear decrease in density is observed with increasing temperature. The differences between the ZnO14-EG and ZnO25-EG nanofluids are small and within the relative uncertainties, meaning that the average size of the ZnO nanoparticles can be considered not to affect the density of the nanofluids. The results of the density values of the MgO-EG nanofluids showed the smallest increase in density compared to the other nanofluids investigated in this work. In_2O_3-EG nanofluids show the greatest increase in density values with increasing nanoparticle concentration with respect to the base fluid and in comparison to the other nanofluids examined in this study. Nevertheless, considering both concentration and temperature increase, all nanofluids show the same behaviour.

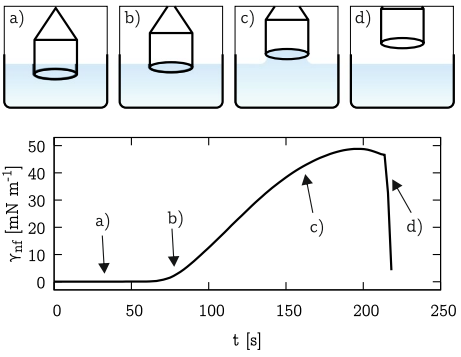

Fig. 2 Measurement process using the Du Noüy ring method as the measured surface tension increases with time. Points marked on the figure represent the position of the ring, (a) ring immersed in the sample, (b) ring at the gas-liquid interface, (c) ring merging from the liquid, (d) breaking contact with the liquid

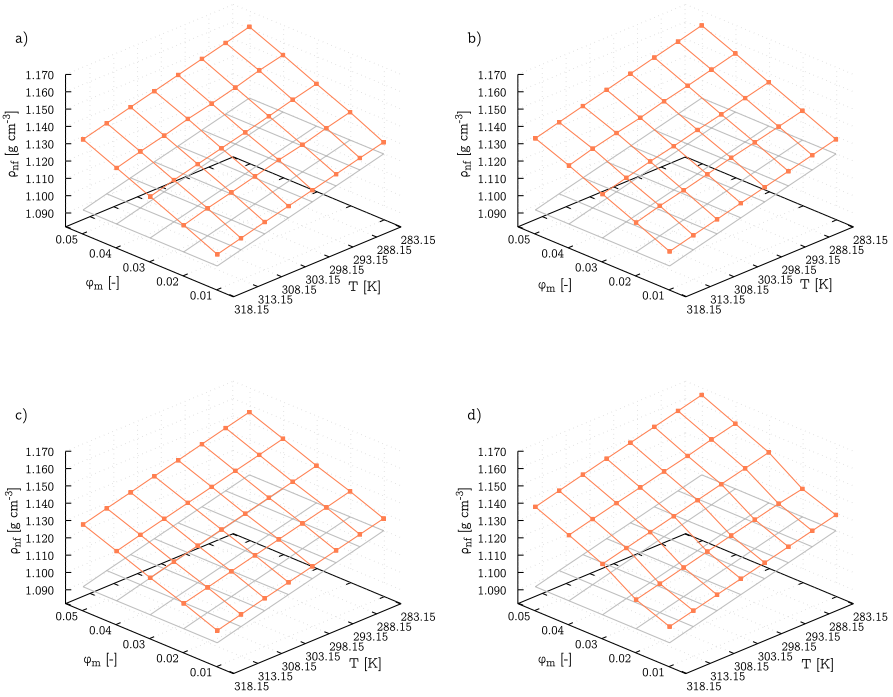

Fig. 3 Dependence of the value of density, ρ_{nf}, on the temperature, T, and the mass fraction, φ_m, of the particles for nanofluids: (a) ZnO14-EG, (b) ZnO25-EG, (c) MgO-EG, (d) In_2O_3-EG. Grey grid present the values of density for pure ethylene glycol

3.2 Surface Tension

The measured surface tension values of all nanofluids investigated in this work are presented in the tables in Appendix 1. In Fig.4, the surface tension values for ZnO14-EG, ZnO25-EG, MgO-EG, In_2O_3-EG nanofluids, and pure ethylene glycol are shown. An increase in surface tension values relative to pure glycol can be observed for all nanofluids. As with previous studies on the surface tension of nanofluids, the ones investigated in this work also show an increase in the surface tension value relative to the pure base fluid but this increase is constant despite the increase in the mass concentration of the nanoparticles. The surface tension values for a temperature of 298.15 K as a function of mass concentration are shown in Fig.5. It can be seen that all the nanofluids tested oscillate around their average values.

The ZnO14-EG nanofluid has an average surface tension value of 48.685 $mN{\cdot}m^{-1}$, this translates into the largest increase in surface tension value relative to the pure base fluid, with a value of 0.648 $mN{\cdot}m^{-1}$. The use of larger nanoparticles in the ZnO25-EG nanofluid resulted, at 298.15 K, in an average increase of 0.434 $mN{\cdot}m^{-1}$ and the average surface tension was 48.471 $mN{\cdot}m^{-1}$. From these results, it can be concluded that in the case of zinc oxide in ethylene glycol nanofluids, the smaller size of the nanoparticles results in a significantly larger increase in the surface tension of the base fluid. The smallest increase stands out for MgO-EG at 298.15 K is an average of 0.298 $mN{\cdot}m^{-1}$ with respect to pure

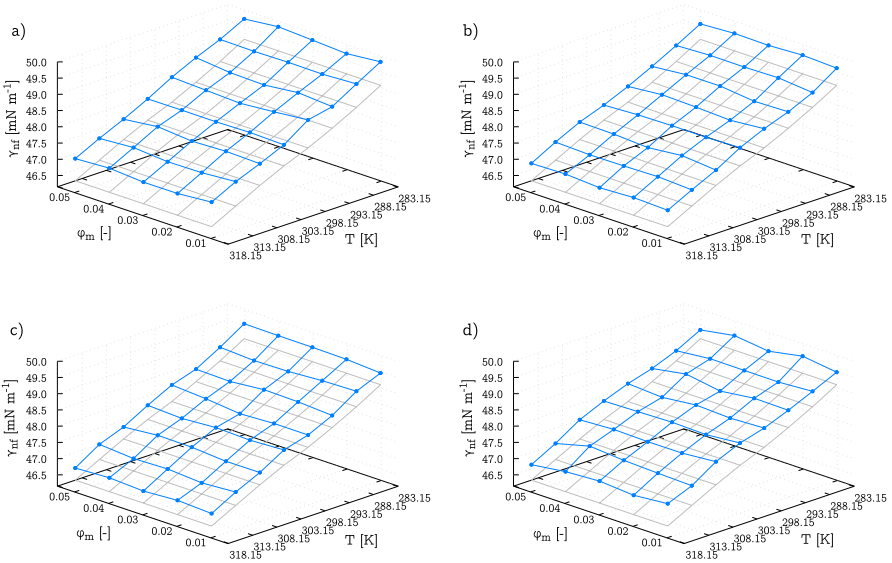

Fig. 4 Dependence of the value of surface tension, γ_{nf}, on the temperature, T, and the mass fraction, φ_m, of the particles for nanofluids: a ZnO14-EG, b ZnO25-EG, c MgO-EG, d In_2O_3-EG. Grey grid present the values of density for pure ethylene glycol

ethylene glycol and the average value was 48.335 mN·m^{-1}. The average surface tension value for the In_2O_3-EG nanofluid at 298.15 K is 48.462 mN·m^{-1} which translates into an average increase of 0.425 mN·m^{-1} with respect to the base fluid.

In previous work [36], it was presented the maximum surface tension value of indium oxide and zinc oxide nanofluids in ethylene glycol using the model

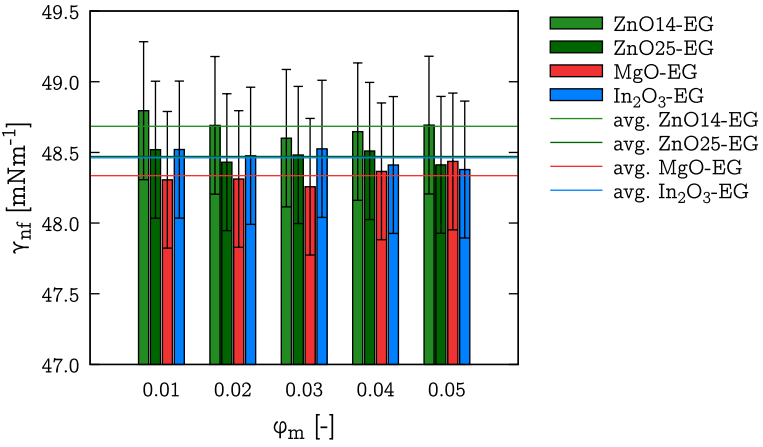

Fig. 5 Comparison of surface tension values for tested ZnO14-EG (light green), ZnO25-EG (green), MgO-EG (red), In_2O_3-EG (blue) nanofluids as a function of nanoparticle mass concentration at 298.15 K. The lines represent the averaged surface tension values for the nanofluids tested

proposed there. The boundary surface tension values at 298.15 K obtained in that work were 48.485 mN·m^{-1} and 48.682 mN·m^{-1} for In_2O_3-EG and ZnO14-EG, respectively. Comparing these values to those obtained in this work, we obtain differences of 0.003 mN·m^{-1} and 0.023 mN·m^{-1} for ZnO14-EG and In_2O_3-EG, respectively. The proposed model of surface tension of nanofluids in Ref. [36], which represents a formula:

$$\gamma_{nf} = \gamma_{bf} + A\left(1 - \frac{1}{e^{\frac{(\varphi_m - C)}{B}} + 1}\right), \tag{1}$$

where γ_{bf} is the value of the surface tension of the base fluid, φ_m is mass fraction, A, B and C are adjustable parameters, is confirmed with reported here data. The average surface tension values of the investigated nanofluids, shown in Fig.5, represent the maximum surface tension values. The determined values of the increase in surface tension relative to the base fluid are the A parameter for a given nanofluid.

4 Conclusions

This paper summarises the results of an experimental study of the density and surface tension of ethylene glycol-based nanofluids with indium oxide, magnesium oxide and zinc oxide.

As shown, densities of ZnO14-EG and ZnO25-EG are comparable from which it can be concluded that the average nanoparticle size of ZnO does not affect the density of these nanofluids. Nevertheless, considering both the concentration and the temperature increase, all tested nanofluids show the same behaviour. The mass density increases linearly with increasing nanoparticle mass fraction and, at the same time, a linear decrease in density is observed with increasing temperature.

The surface tension of studied nanofluids follows the model proposed in the paper [36], which assumes saturation of the surface of the base fluid with nanoparticles. The averaged surface tension values for the studied ZnO14-EG, ZnO25-EG, MgO-EG, In_2O_3-EG nanofluids at 298.15 K are 48.685, 48.471, 48.335, and 48.462 mN·m^{-1}, respectively.

Future works on the surface tension of nanofluids should be focused on the experimental examination of the values of γ for various types of nanofluids, and based on this data along with the model presented in Ref. [36] a comprehensive study on the liquid-particle-gas interactions could be build.

Appendix 1

See Tables 1, 2, 3, 4.

Table 1 Experimental values of the density, ρ, and surface tension, γ, of ZnO14-EG nanofluids at pressure $p = 0.10$ MPa and various temperatures from $T = 283.15$ K to $T = 318.15$ K and different of mass fractions of nanoparticles, φ_m

T (K)→	283.15	288.15	293.15	298.15	303.15	308.15	313.15	318.15
φ_m (-)	ρ (g·cm^{-3})							
0.00	1.1202	1.1167	1.1133	1.1098	1.1063	1.1028	1.0992	1.0957
0.01	1.1270	1.1236	1.1200	1.1165	1.1130	1.1095	1.1059	1.1023
0.02	1.1363	1.1328	1.1289	1.1258	1.1221	1.1185	1.1151	1.1111
0.03	1.1445	1.1411	1.1373	1.1337	1.1303	1.1268	1.1233	1.1195
0.04	1.1531	1.1499	1.1458	1.1422	1.1391	1.1352	1.1317	1.1279
0.05	1.1613	1.1577	1.1542	1.1507	1.1471	1.1436	1.1400	1.1364
φ_m (-)	γ (mN m^{-1})							
0.00	49.121	48.778	48.386	48.037	47.631	47.275	46.882	46.499
0.01	49.833	49.403	48.954	48.795	48.274	47.944	47.642	47.261
0.02	49.731	49.351	49.030	48.691	48.303	47.972	47.564	47.175
0.03	49.793	49.362	48.912	48.601	48.280	47.931	47.548	47.168
0.04	49.853	49.345	48.941	48.647	48.284	48.024	47.630	47.247
0.05	49.740	49.357	49.048	48.693	48.278	47.900	47.559	47.187

The estimated standard relative uncertainty $u_r(\varphi_m) = 0.01$, $u_r(\rho) = 0.001$, $u_r(\gamma) = 0.01$, $u(p) = 0.01$ MPa and $u(T) = 0.10$ K

Table 2 Experimental values of the density, ρ, and surface tension, γ, of ZnO25-EG nanofluids at pressure $p = 0.10$ MPa and various temperatures from $T = 283.15$ K to $T = 318.15$ K and different of mass fractions of nanoparticles, φ_m

T (K)→	283.15	288.15	293.15	298.15	303.15	308.15	313.15	318.15
φ_m (-)	ρ (g·cm^{-3})							
0.00	1.1202	1.1167	1.1133	1.1098	1.1063	1.1028	1.0992	1.0957
0.01	1.1287	1.1252	1.1217	1.1182	1.1147	1.1111	1.1076	1.1040
0.02	1.1371	1.1337	1.1303	1.1271	1.1233	1.1198	1.1165	1.1126
0.03	1.1455	1.1421	1.1384	1.1351	1.1315	1.1283	1.1246	1.1209
0.04	1.1540	1.1504	1.1468	1.1436	1.1398	1.1367	1.1334	1.1293
0.05	1.1621	1.1585	1.1550	1.1514	1.1478	1.1442	1.1406	1.1370
φ_m (-)	γ (mN m^{-1})							
0.00	49.121	48.778	48.386	48.037	47.631	47.275	46.882	46.499
0.01	49.638	49.136	48.793	48.519	48.188	47.744	47.387	47.010
0.02	49.682	49.237	48.765	48.431	48.154	47.841	47.440	47.048
0.03	49.630	49.214	48.881	48.482	48.156	47.733	47.417	46.997
0.04	49.647	49.222	48.875	48.510	48.139	47.796	47.408	47.066
0.05	49.586	49.170	48.777	48.412	48.087	47.815	47.444	47.038

The estimated standard relative uncertainty $u_r(\varphi_m) = 0.01$, $u_r(\rho) = 0.001$, $u_r(\gamma) = 0.01$, $u(p) = 0.01$ MPa and $u(T) = 0.10$ K

Table 3 Experimental values of the density, ρ, and surface tension, γ, of MgO-EG nanofluids at pressure $p = 0.10$ MPa and various temperatures from $T = 283.15$ K to $T = 318.15$ K and different of mass fractions of nanoparticles, φ_m

T / K →	283.15	288.15	293.15	298.15	303.15	308.15	313.15	318.15
φ_m (-)	ρ (g·cm^{-3})							
0.00	1.1202	1.1167	1.1133	1.1098	1.1063	1.1028	1.0992	1.0957
0.01	1.1273	1.1238	1.1203	1.1168	1.1133	1.1098	1.1062	1.1027
0.02	1.1349	1.1313	1.1278	1.1243	1.1208	1.1173	1.1137	1.1102
0.03	1.1416	1.1381	1.1346	1.1311	1.1276	1.1240	1.1205	1.1169
0.04	1.1491	1.1455	1.1402	1.1385	1.1305	1.1315	1.1279	1.1243
0.05	1.1564	1.1529	1.1494	1.1458	1.1423	1.1387	1.1352	1.1316
φ_m (-)	γ (mN·m^{-1})							
0.00	49.121	48.778	48.386	48.037	47.631	47.275	46.882	46.499
0.01	49.464	49.157	48.661	48.306	48.097	47.651	47.300	46.889
0.02	49.537	49.128	48.726	48.312	48.044	47.646	47.229	46.941
0.03	49.552	49.059	48.748	48.257	48.079	47.724	47.305	46.875
0.04	49.558	49.039	48.648	48.366	48.012	47.738	47.272	46.929
0.05	49.569	49.096	48.672	48.436	48.060	47.639	47.354	46.876

The estimated standard relative uncertainty $u_r(\varphi_m) = 0.01$, $u_r(\rho) = 0.001$, $u_r(\gamma) = 0.01$, $u(p) = 0.01$ MPa and $u(T) = 0.10$ K

Table 4 Experimental values of the density, ρ, and surface tension, γ, of In_2O_3-EG nanofluids at pressure $p = 0.10$ MPa and various temperatures from $T = 283.15$ K to $T = 318.15$ K and different of mass fractions of nanoparticles, φ_m

T / K →	283.15	288.15	293.15	298.15	303.15	308.15	313.15	318.15
φ_m (-)	ρ (g·cm^{-3})							
0.00	1.1202	1.1167	1.1133	1.1098	1.1063	1.1028	1.0992	1.0957
0.01	1.1294	1.1259	1.1224	1.1189	1.1154	1.1119	1.1084	1.1049
0.02	1.1363	1.1335	1.1300	1.1265	1.1230	1.1195	1.1159	1.1124
0.03	1.1493	1.1458	1.1424	1.1389	1.1354	1.1319	1.1284	1.1249
0.04	1.1578	1.1544	1.1506	1.1474	1.1439	1.1406	1.1371	1.1335
0.05	1.1663	1.1628	1.1593	1.1559	1.1524	1.1489	1.1454	1.1418
φ_m (-)	γ (mN·m^{-1})							
0.00	49.121	48.778	48.386	48.037	47.631	47.275	46.882	46.499
0.01	49.492	49.152	48.819	48.520	48.311	47.986	47.495	47.194
0.02	49.633	49.086	48.837	48.476	48.216	47.897	47.529	47.099
0.03	49.432	49.090	48.706	48.525	48.248	47.893	47.572	47.181
0.04	49.561	49.096	48.874	48.411	48.218	47.917	47.654	47.118
0.05	49.381	48.991	48.694	48.479	48.191	47.866	47.382	46.979

The estimated standard relative uncertainty $u_r(\varphi_m) = 0.01$, $u_r(\rho) = 0.001$, $u_r(\gamma) = 0.01$, $u(p) = 0.01$ MPa and $u(T) = 0.10$ K

Author Contributions Conceptualization: J.T. and G.Ż.; Data curation: J.T.; Formal analysis: J.T.; Investigation: J.T.; Methodology: J.T. and G.Ż.; Project administration: G.Ż.; Resources: G.Ż.; Software: J.T.; Supervision: G.Ż.; Validation: J.T. and G.Ż.; Visualization: J.T.; Writing - original draft: J.T.; Writing - review & editing: G.Ż. All authors reviewed the manuscript.

Funding Not applicable.

Data Availability All data generated or analysed during this study are included in this published article.

Declarations

Competing Interests The authors declare they have no competing interests.

Ethical Approval Not applicable.

References

1. L. Qiu, N. Zhu, Y. Feng, E.E. Michaelides, G. Żyła, D. Jing, X. Zhang, P.M. Norris, C.N. Markides, O. Mahian, A review of recent advances in thermophysical properties at the nanoscale: from solid state to colloids. Phys. Rep. **843**, 1–81 (2020)
2. J.P. Vallejo, J.I. Prado, L. Lugo, Hybrid or mono nanofluids for convective heat transfer applications. A critical review of experimental research. Appl. Thermal Eng. **203**, 117926 (2021)
3. A. Can, F. Selimefendigil, H.F. Öztop, A review on soft computing and nanofluid applications for battery thermal management. J. Energy Storage **53**, 105214 (2022)
4. S.P. Tembhare, D.P. Barai, B.A. Bhanvase, Performance evaluation of nanofluids in solar thermal and solar photovoltaic systems: a comprehensive review. Renew. Sustain. Energy Rev. **153**, 111738 (2022)
5. H. Lin, Q. Jian, X. Bai, D. Li, Z. Huang, W. Huang, S. Feng, Z. Cheng. Recent advances in thermal conductivity and thermal applications of graphene and its derivatives nanofluids. Appl. Therm. Eng. 119176 (2022)
6. M.A. Abdelkareem, M.S. Mahmoud, K. Elsaid, E.T. Sayed, T. Wilberforce, M. Al-Murisi, H.M. Maghrabie, A.G. Olabi, Prospects of thermoelectric generators with nanofluid. Therm. Sci. Eng. Progress **29**, 101207 (2022)
7. A. Rafiei, R. Loni, S.B. Mahadzir, G. Najafi, M. Sadeghzadeh, M. Mazlan, M.H. Ahmadi, Hybrid solar desalination system for generation electricity and freshwater with nanofluid application: Energy, exergy, and environmental aspects. Sustain. Energy Technol. Assess. **50**, 101716 (2022)
8. M. Hussain, F.A. Mir, M.A. Ansari, Nanofluid transformer oil for cooling and insulating applications: a brief review. Appl. Surf. Sci. Adv. **8**, 100223 (2022)
9. M. Gürdal, K. Arslan, E. Gedik, A.A. Minea, Effects of using nanofluid, applying a magnetic field, and placing turbulators in channels on the convective heat transfer: A comprehensive review. Renew. Sustain. Energy Rev. **162**, 112453 (2022)
10. A. Joseph, J. Sobczak, G. Żyła, S. Mathew, Ionic liquid and ionanofluid-based redox flow batteries-a mini review. Energies **15**, 4545 (2022)
11. Yu. Wei, H. Xie, L. Chen, Y. Li, Investigation of thermal conductivity and viscosity of ethylene glycol based ZnO nanofluid. Thermochim. Acta **491**(1–2), 92–96 (2009)

12. M.J. Pastoriza-Gallego, L. Lugo, D. Cabaleiro, J.L. Legido, M.M. Piñeiro, Thermophysical profile of ethylene glycol-based ZnO nanofluids. J. Chem. Thermodyn. **73**, 23–30 (2014)
13. K.S. Suganthi, V.L. Vinodhan, K.S. Rajan, Heat transfer performance and transport properties of ZnO–ethylene glycol and ZnO–ethylene glycol–water nanofluid coolants. Appl. Energy **135**, 548–559 (2014)
14. H. Li, L. Wang, Y. He, H. Yanwei, J. Zhu, B. Jiang, Experimental investigation of thermal conductivity and viscosity of ethylene glycol based ZnO nanofluids. Appl. Therm. Eng. **88**, 363–368 (2015)
15. A.B. Demirpolat, M. Baykara, Investigation and prediction of ethylene glycol based ZnO nanofluidic heat transfer versus magnetic effect by deep learning. Thermal Sci. Eng. Prog. **25**, 101034 (2021)
16. H. Xie, Yu. Wei, W. Chen, Mgo nanofluids: higher thermal conductivity and lower viscosity among ethylene glycol-based nanofluids containing oxide nanoparticles. J. Exp. Nanosci. **5**, 463–472 (2010)
17. M. Hemmat Esfe, S. Saedodin, M. Bahiraei, D. Toghraie, O. Mahian, S. Wongwises, Thermal conductivity modeling of MgO/EG nanofluids using experimental data and artificial neural network. J. Therm. Anal. Calorim. **118**, 287–294 (2014)
18. S.A. Adio, M. Sharifpur, J.P. Meyer, Factors affecting the ph and electrical conductivity of MgO-ethylene glycol nanofluids. Bull. Mater. Sci. **38**, 1345–1357 (2015)
19. S.A. Adio, M. Mehrabi, M. Sharifpur, J.P. Meyer, Experimental investigation and model development for effective viscosity of MgO-ethylene glycol nanofluids by using dimensional analysis, fcm-anfis and ga-pnn techniques. Int. Commun. Heat Mass Transfer **72**, 71–83 (2016)
20. G. Żyła, J. Fal, Viscosity, thermal and electrical conductivity of silicon dioxide-ethylene glycol transparent nanofluids: an experimental studies. Thermochim. Acta **650**, 106–113 (2017)
21. J. Fal, M. Wanic, M. Malick, M. Oleksy, G. Żyła, Experimental investigation of electrical conductivity of ethylene glycol containing indium oxide nanoparticles. Actaphys. Polon. A **135**, 1237–1239 (2019)
22. G. Żyła, M. Wanic, M. Malicka, J. Fal, Dynamic viscosity of indium oxide-ethylene glycol (In_2O_3-EG) nanofluids: an experimental investigation. Acta Phys. Pol A **135**, 1290–3 (2019)
23. P. Estellé, D. Cabaleiro, G. Żyła, L. Lugo, S.M.S. Murshed, Current trends in surface tension and wetting behavior of nanofluids. Renew. Sustain. Energy Rev. **94**, 931–944 (2018)
24. B.H. Kim, G.P. Peterson, Analysis of the critical weber number at the onset of liquid entrainment in capillary-driven heat pipes. Int. J. Heat Mass Transf. **38**, 1427–1442 (1995)
25. P. Terdtoon, M. Shiraishi, M. Murakami, Effect of inclination angle on heat transfer characteristics of closed two-phase thermosyphon, in *Proc. 7th Int. Heat Pipe Conf* (1990)
26. I. Golobič, B. Gašperšič, Corresponding states correlation for maximum heat flux in two-phase closed thermosyphon. Int. J. Refrig. **20**, 402–410 (1997)
27. S.G. Kandlikar, Heat transfer mechanisms during flow boiling in microchannels. J. Heat Transf. **126**, 8–16 (2004)
28. J. Traciak, J. Sobczak, R. Kuzioła, J. Wasag, G. Żyła, Surface and optical properties of ethylene glycol-based nanofluids containing silicon dioxide nanoparticles: an experimental study. J. Therm. Anal. Calorim. **147**, 7665–7673 (2022)
29. J. Traciak, J. Sobczak, G. Żyła, The experimental study of the surface tension of titanium dioxide-ethylene glycol nanofluids. Physica E **145**, 115494 (2023)
30. J. Traciak, J. Sobczak, J.P. Vallejo, L. Lugo, J. Fal, G. Żyła, Experimental study on the density, surface tension and electrical properties of ZrO_2-EG nanofluids. Phys. Chem. Liquids, 1–11 (2022)
31. M. Moosavi, E.K. Goharshadi, A. Youssefi, Fabrication, characterization, and measurement of some physicochemical properties of ZnO nanofluids. Int. J. Heat Fluid Flow **31**, 599–605 (2010)
32. M. Wanic, D. Cabaleiro, S. Hamze, J. Fal, P. Estellé, G. Żyła, Surface tension of ethylene glycol-based nanofluids containing various types of nitrides. J. Therm. Anal. Calorim. **139**, 799–806 (2020)
33. G. Żyła, J. Fal, P. Estellé, Thermophysical and dielectric profiles of ethylene glycol based titanium nitride (TiN-EG) nanofluids with various size of particles. Int. J. Heat Mass Transf. **113**, 1189–1199 (2017)
34. A.R. Harikrishnan, P. Dhar, P.K. Agnihotri, S. Gedupudi, S.K. Das, Effects of interplay of nanoparticles, surfactants and base fluid on the surface tension of nanocolloids. Eur. Phys. J. E **40**, 1–14 (2017)

35. J. Traciak, J. Fal, G. Żyła, 3D printed measuring device for the determination the surface tension of nanofluids. Appl. Surf. Sci., 149878 (2021)
36. J. Traciak, G. Żyła, Effect of nanoparticles saturation on the surface tension of nanofluids. J. Mol. Liq. **363**, 119937 (2022)
37. H. Zuidema, G. Waters, Ring method for the determination of interfacial tension. Ind. Eng. Chem. Anal. Edn. **13**, 312–313 (1941)
38. F. Steckel, S. Szapiro, Physical properties of heavy oxygen water. Part 1. Density and thermal expansion. Trans. Faraday Soc. **59**, 331–343 (1963)
39. S. Azizian, N. Bashavard, Equilibrium surface tensions of benzyl alcohol+ethylene glycol mixtures. J. Chem. Eng. Data **50**, 709–712 (2005)
40. A.A. Rafati, E. Ghasemian, M. Abdolmaleki, Surface properties of binary mixtures of ethylene glycol with a series of aliphatic alcohols (1-pentanol, 1-hexanol, and 1-heptanol). J. Chem. Eng. Data **53**, 1944–1949 (2008)